Segmental Orientation in Uniaxially Deformed Networks: A Higher Order Approximation for Finite Chains and Large Deformations

Burak Erman,* Turkan Haliloglu, and Ivet Bahar

Polymer Research Center and School of Engineering, Bogazici University, Bebek 80815, Istanbul, Turkey

James E. Mark

Polymer Research Center and Department of Chemistry, University of Cincinnati, Cincinnati, Ohio 45221

Received June 5, 1990

ABSTRACT: The orientation of a reference vector **m** rigidly embedded in a chain of a deformed network is considered. As a first step, following Nagai's earlier treatment, the mean-square cosine $\langle\cos^2\theta\rangle_{\mathbf{r}}$ of the angle that **m** makes with a laboratory-fixed axis is formulated for a chain with fixed end-to-end vector **r**. An expression including terms up to fifth inverse power of n, where n is the number of bonds in the network chain, is obtained for $\langle\cos^2\theta\rangle_{\mathbf{r}}$. Next, the corresponding average over all chains of a network and the associated orientation function, S, are found in terms of (i) unperturbed chain moments readily obtainable by the rotational isomeric state scheme and (ii) the extension ratio for uniaxially deformed networks. Such a rigorous expression for S is particularly useful for relatively short chains and for moderate to large deformations that cannot be satisfactorily accounted for by existing simpler formulations. Thus, we estimate ranges of extension ratios λ to which the conventional first-order approximation may be confidently applied. Calculations performed for polyethylene chains with n = 20–100 gave results that could be compared with those obtained in Monte Carlo simulations and previous theoretical approaches. These comparisons demonstrate the importance of adoption of a higher order approximation for the orientation function for $\lambda \geq 1.8$.

Introduction

Theoretical characterization of segmental orientation in polymeric chains subject to an external disturbance is based almost entirely on the freely jointed chain model. Although this model conveniently leads to simple analytical expressions for segmental orientation, its inadequacy to reflect the effects of the real chemical structure of a specific polymeric system is a serious weakness resulting from its utmost simplicity. Recent developments in spectroscopic experimental techniques, in particular, the use of dynamic infrared spectroscopy[1] and deuterium NMR spectroscopy,[2] permit very accurate measurement of segmental orientation in polymeric systems in the deformed state. The degree of accuracy of these two techniques is unprecedented by any of the conventional techniques of measurement in this field.

On the theoretical side, the general formulation of the problem of segmental orientation in real chains has been outlined in the pioneering work of Nagai.[3] Calculation methods for segmental orientation according to the rotational isomeric scheme for real chains were later improved by Flory[4] in a form that is more suitable for the study of birefringence. The formulations of both Nagai and Flory lead to an expression in the form of a series expansion containing various-order moments of the chain end-to-end vector and related trigonometric variables. For sufficiently long chains, i.e., chains containing more than 100 bonds, the first term of the series is sufficient for a reasonable representation. However, as the number of bonds decreases, more terms of the series are required for accuracy. The specific aim of the present study is to give a more rigorous expression for the orientation function that includes several powers of $1/n$, where n is the number of bonds of the chain. By the use of such an expression, the relative contributions of the first- and second-order approximations to segmental orientation are assessed. It should be noted, at this point, that the original paper of Nagai contains some minor printing mistakes in the expression for orientation and not all of the sixth-order terms are included therein. The treatment by Flory, on the other hand, is developed only for birefringence and is not exactly suitable for the study of segmental orientation. The present treatment may thus be regarded as an improvement and completion of the previous formulations of Nagai and Flory.

We adopt the affine model of a network. The choice of a network for describing segmental orientation is only for the convenience of visualizing the chains in equilibrium in the deformed state. We therefore assume each chain to extend between two active junctions that displace affinely with the macroscopic deformation. The treatment may be applied to systems other than networks by suitably assuming two points on the chain to deform affinely and calculating the state of segmental orientation between those two points. In this respect the present treatment focuses only on intramolecular contributions to segmental orientation. Intermolecular contributions imposed by the local anisotropic environment of a given segment are not considered.

Theory

One configuration of a single chain is shown in Figure 1. $Oxyz$ represents a laboratory-fixed coordinate system. The two ends of the chain at O and A represent points fixed in space. In a network, those are the two junction points at the termini of a network chain. They are assumed to displace affinely with the macroscopic deformation. **r** in the figure represents the end-to-end vector of the chain in the deformed state, which, in the undeformed state, is equal to $\mathbf{r}_0$. For simple elongation along the x direction, using the deformation gradient tensor λ, we have

$$\mathbf{r} = \lambda\mathbf{r}_0 \tag{1}$$

0024-9297/91/2224-0901$02.50/0

where

$$\lambda = \begin{bmatrix} x/x_0 & 0 & 0 \\ 0 & y/y_0 & 0 \\ 0 & 0 & z/z_0 \end{bmatrix} = \begin{bmatrix} \lambda & 0 & 0 \\ 0 & \lambda^{-1/2} & 0 \\ 0 & 0 & \lambda^{-1/2} \end{bmatrix} \quad (2)$$

with x_0, y_0, and z_0 and x, y, and z denoting the components of $\mathbf{r}_0$ and $\mathbf{r}$, respectively, and λ representing the extension ratio.

In Figure 1, $\mathbf{m}$ represents a unit vector rigidly affixed to the chain at a given point. It makes an angle θ with the x axis as shown. In the present treatment, $\mathbf{m}$ may represent the direction of any sequence of bonds in the chain or it may refer to a specific label attached to the chain. Identification of $\mathbf{m}$ with one of the principal components of the optical polarizability tensor provides the basis for the analysis of strain birefringence,[4] whereas in the treatment of the dichroic ratio, it is identified with the absorption transition moment of the excited group. We are interested in the orientation of $\mathbf{m}$ as the network deforms and the ends of the chain displace affinely with macroscopic strain.

The orientation of $\mathbf{m}$ will be calculated in two stages: In the first stage, we consider only a single chain whose end-to-end vector $\mathbf{r}$ is fixed in space and calculate the average $\langle\cos^2\theta\rangle_\mathbf{r}$ over all configurations of that chain. Here, the subscript $\mathbf{r}$ refers to the averaging over all configurations at fixed $\mathbf{r}$. In the second stage, we find the average $\langle\cos^2\theta\rangle$ over all chains of the system. Here, the subscript $\mathbf{r}$ is deleted inasmuch as the constraint of fixed $\mathbf{r}$ is removed.

Step 1. Calculation of $\langle\cos^2\theta\rangle_\mathbf{r}$. We follow a procedure similar to but not identical with the one adopted by Nagai[3] and Flory.[4] The average $\langle\cos^2\theta\rangle_\mathbf{r}$ is expressed by

$$\langle\cos^2\theta\rangle_\mathbf{r} = Z_\mathbf{r}^{-1}\int \cos^2\theta \exp(-E\{\phi\}_\mathbf{r}/kT)\, d\{\phi\}_\mathbf{r} \quad (3)$$

where $E\{\phi\}_\mathbf{r}$ is the energy of the configuration $\{\phi\}_\mathbf{r}$, which is defined by a set of skeletal bond rotations. The subscript $\mathbf{r}$ in $d\{\phi\}_\mathbf{r}$ indicates that the integration is carried out over only those configurations that possess the specified end-to-end vector $\mathbf{r}$. It should be understood that the whole configurational space is referred to whenever the subscript $\mathbf{r}$ is omitted. k is the Boltzmann factor, and T is the absolute temperature. $Z_\mathbf{r}$ is the configuration partition function for a chain with fixed $\mathbf{r}$, defined as

$$Z_\mathbf{r} = \int \exp(-E\{\phi\}_\mathbf{r}/kT)\, d\{\phi\}_\mathbf{r} \quad (4)$$

Denoting the integral in the right-hand side of eq 3 by $f(\mathbf{r})$, we have

$$f(\mathbf{r}) \equiv \int \cos^2\theta \exp(-E\{\phi\}_\mathbf{r}/kT)\, d\{\phi\}_\mathbf{r} = \langle\cos^2\theta\rangle_\mathbf{r} Z_\mathbf{r} \quad (5)$$

The Fourier transform $f(\mathbf{q})$ of $f(\mathbf{r})$ is

$$f(\mathbf{q}) = \int e^{-i\mathbf{q}\cdot\mathbf{r}}\langle\cos^2\theta\rangle_\mathbf{r} Z_\mathbf{r}\, d\mathbf{r} \quad (6)$$

$$f(\mathbf{q}) = \int_r\int_{\chi,\psi,\omega}\int_{|\phi|_\mathbf{r}} \cos^2\theta \times \exp(-E\{\phi\}_\mathbf{r}/kT)e^{-i\mathbf{q}\cdot\mathbf{r}} \sin\chi\, d\chi\, d\psi\, d\omega\, d\{\phi\}_\mathbf{r}\, dr \quad (7)$$

Here $\mathbf{q}$ is the transform variable, r is the magnitude of $\mathbf{r}$, and χ, ψ, and ω are the three Euler angles defined in Figure 2. In this figure, XYZ is a new Cartesian coordinate system with the Z axis parallel to $\mathbf{q}$, and the X axis is in the xZ plane. The X axis makes an acute angle with x. χ and ψ are the polar and azimuthal angles, respectively, locating $\mathbf{r}$ relative to $\mathbf{q}$ along the polar axis Z. ω gives the rotation of the plane defined by $\mathbf{m}$ and $\mathbf{r}$ from the plane of $\mathbf{r}$ and Z. Using

$$\int_r\int_{\chi,\psi,\omega}\int_{|\phi|_\mathbf{r}} d\{\phi\}_\mathbf{r} \sin\chi\, d\chi\, d\psi\, d\omega\, dr = 8\pi^2\int_r\int_{|\phi|_\mathbf{r}} d\{\phi\}_\mathbf{r}\, dr = \int_\mathbf{r}\int_{|\phi|_\mathbf{r}} d\{\phi\}_\mathbf{r}\, d\mathbf{r} = \int_{|\phi|} d\{\phi\} \quad (8)$$

eq 7 may be rewritten as

$$f(\mathbf{q}) = (8\pi^2)^{-1}\int_{|\phi|}\cos^2\theta \times \exp(-E\{\phi\}/kT)e^{-i\mathbf{q}\cdot\mathbf{r}} \sin\chi\, d\chi\, d\psi\, d\omega\, d\{\phi\} \quad (9)$$

Let Φ denote the angle between $\mathbf{m}$ and $\mathbf{r}$ as shown in Figure 2a. The laboratory-fixed system $Oxyz$ is shown in part b of the same figure. The components of $\mathbf{q}$ along the x, y, and z axes are indicated as q_x, q_y, and q_z. The angle between the x axis and $\mathbf{q}$ is shown by τ. From the scalar product of $\mathbf{m}$ with the x axis, both of them being expressed in the frame XYZ, it is possible to write $\cos\theta$ in terms of χ, ψ, ω, Φ, and τ as

$$\cos\theta = \sin\tau[\sin\chi\cos\psi\cos\Phi + (\cos\chi\cos\psi\cos\omega - \sin\psi\sin\omega)\sin\Phi] + \cos\tau[\cos\chi\cos\Phi - \sin\chi\cos\omega\sin\Phi] \quad (10)$$

The substitution of eq 10 into eq 9 and integration over χ, ψ, and ω, at fixed $\{\phi\}$, lead to the series expression

$$f(\mathbf{q}) = \frac{1}{3}\int\left[\left[1 - \frac{(qr)^2}{3!} + \frac{(qr)^4}{5!} - \frac{(qr)^6}{7!} + \frac{(qr)^8}{9!} + \ldots\right] - \frac{1}{2}(3\cos^2\tau - 1)(3\cos^2\Phi - 1)\left[\frac{(qr)^2}{5\cdot3} - \frac{(qr)^4}{7\cdot5\cdot3!} + \frac{(qr)^6}{9\cdot7\cdot5!} - \frac{(qr)^8}{11\cdot9\cdot7!} + \ldots\right]\right]\exp(-E/kT)\, d\{\phi\} \quad (11)$$

where q is the magnitude of $\mathbf{q}$. Expressing the internal configuration variables in terms of the configurational averages of the various quantities, we obtain

$$f(\mathbf{q}) = \frac{Z}{3}\left\{\left[1 - \frac{\langle r^2\rangle_0 q^2}{3!} + \frac{\langle r^4\rangle_0 q^4}{5!} - \frac{\langle r^6\rangle_0 q^6}{7!} + \frac{\langle r^8\rangle_0 q^8}{9!} + \ldots\right] - \frac{1}{2}(3q_x^2 - q^2)\left[\frac{1}{5\cdot3}(3\langle r^2\cos^2\Phi\rangle_0 - \langle r^2\rangle_0) - \frac{q^2}{7\cdot5\cdot3!}(3\langle r^4\cos^2\Phi\rangle_0 - \langle r^4\rangle_0) + \frac{q^4}{9\cdot7\cdot5!}(3\langle r^6\cos^2\Phi\rangle_0 - \langle r^6\rangle_0) - \frac{q^6}{11\cdot9\cdot7!}(3\langle r^8\cos^2\Phi\rangle_0 - \langle r^8\rangle_0) + \ldots\right]\right\} \quad (12)$$

where the subscript zero appended to angular brackets refers to the averaging of the chains in the unperturbed state and Z is the configuration partition function for the free chain. Equation 12 is in form identical with the expression that was given by Flory up to sixth-order terms. Following the procedure adopted by Flory, multiplication of the denominator of eq 12 by $\exp(\langle r^2\rangle_0 q^2/6)$ and the numerator by the series expansion of this expression leads to

$$f(\mathbf{q}) = \frac{Z}{3}\exp(-\langle r^2\rangle_0 q^2/6)\{1 + [\eta_2(\langle r^2\rangle_0/3) + \eta_4(\langle r^2\rangle_0/3)^2 q^2 + \eta_6(\langle r^2\rangle_0/3)^3 q^4 + \eta_8(\langle r^2\rangle_0/3)^4 q^6 + \ldots] \times (q^2 - 3q_x^2) + [g_4(\langle r^2\rangle_0/3)^2 q^4 + g_6(\langle r^2\rangle_0/3)^3 q^6 + g_8(\langle r^2\rangle_0/3)^4 q^8 + \ldots]\} \quad (13)$$

where

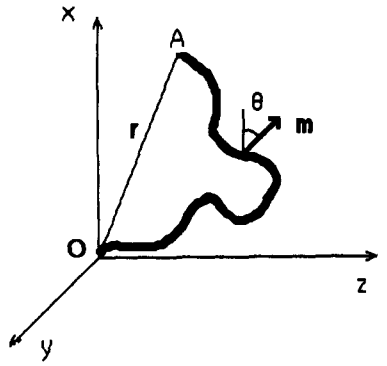

Figure 1. Schematic representation of a chain OA with end-to-end vector **r**. The vector **m** is rigidly affixed to the chain and makes an angle θ with the laboratory-fixed x axis.

$$\eta_2 \equiv \frac{1}{10}\left(\frac{3\langle r^2\cos^2\Phi\rangle_0}{\langle r^2\rangle_0} - 1\right)$$

$$\eta_4 \equiv \frac{1}{20}\left[\left(\frac{3\langle r^2\cos^2\Phi\rangle_0}{\langle r^2\rangle_0} - 1\right) - \frac{3}{7}\left(\frac{3\langle r^4\cos^2\Phi\rangle_0}{\langle r^2\rangle_0^2} - \frac{\langle r^4\rangle_0}{\langle r^2\rangle_0^2}\right)\right]$$

$$\eta_6 \equiv \frac{1}{80}\left[\left(\frac{3\langle r^2\cos^2\Phi\rangle_0}{\langle r^2\rangle_0} - 1\right) - \frac{6}{7}\left(\frac{3\langle r^4\cos^2\Phi\rangle_0}{\langle r^2\rangle_0^2} - \frac{\langle r^4\rangle_0}{\langle r^2\rangle_0^2}\right) + \frac{1}{7}\left(\frac{3\langle r^6\cos^2\Phi\rangle_0}{\langle r^2\rangle_0^3} - \frac{\langle r^6\rangle_0}{\langle r^2\rangle_0^3}\right)\right]$$

$$\eta_8 \equiv \frac{1}{480}\left[\left(\frac{3\langle r^2\cos^2\Phi\rangle_0}{\langle r^2\rangle_0} - 1\right) - \frac{9}{7}\left(\frac{3\langle r^4\cos^2\Phi\rangle_0}{\langle r^2\rangle_0^2} - \frac{\langle r^4\rangle_0}{\langle r^2\rangle_0^2}\right) + \frac{3}{7}\left(\frac{3\langle r^6\cos^2\Phi\rangle_0}{\langle r^2\rangle_0^3} - \frac{\langle r^6\rangle_0}{\langle r^2\rangle_0^3}\right) - \frac{3}{77}\left(\frac{3\langle r^8\cos^2\Phi\rangle_0}{\langle r^2\rangle_0^4} - \frac{\langle r^8\rangle_0}{\langle r^2\rangle_0^4}\right)\right] \quad (14)$$

and

$$g_4 \equiv -\left(\frac{1}{2!2^2}\right)\left[1 - \frac{3\langle r^4\rangle_0}{5\langle r^2\rangle_0^2}\right]$$

$$g_6 \equiv -\left(\frac{1}{3!2^3}\right)\left[3\left(1 - \frac{3\langle r^4\rangle_0}{5\langle r^2\rangle_0^2}\right) - \left(1 - \frac{3^2\langle r^6\rangle_0}{5\cdot 7\langle r^2\rangle_0^3}\right)\right]$$

$$g_8 \equiv -\left(\frac{1}{4!2^4}\right)\left[6\left(1 - \frac{3\langle r^4\rangle_0}{5\langle r^2\rangle_0^2}\right) - 4\left(1 - \frac{3^2\langle r^6\rangle_0}{5\cdot 7\langle r^2\rangle_0^3}\right) + \left(1 - \frac{3^3\langle r^8\rangle_0}{5\cdot 7\cdot 9\langle r^2\rangle_0^4}\right)\right] \quad (15)$$

The inverse Fourier transform of eq 6 yields the required average

$$\langle\cos^2\theta\rangle_{\mathbf{r}} = (2\pi)^{-3}Z_{\mathbf{r}}^{-1}\int f(\mathbf{q})e^{i\mathbf{q}\cdot\mathbf{r}}\,d\mathbf{q} \quad (16)$$

Substituting from eq 13 into eq 16, writing $\mathbf{q}\cdot\mathbf{r}$ as $xq_x + yq_y + zq_z$, and performing the integrations lead to

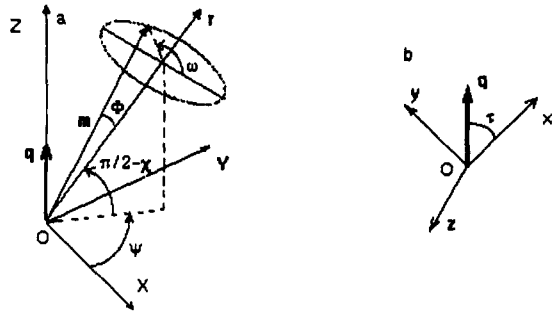

Figure 2. (a) Representation of **m** and **r** in the XYZ coordinate system in which the Z axis is parallel to the transform variable **q**. Φ is the angle between **m** and **r**. ψ, χ, and ω are the three Euler angles. (b) Position of the transform variable **q** with respect to the laboratory-fixed frame xyz. τ is the angle it makes with the x axis.

$$\langle\cos^2\theta\rangle_{\mathbf{r}} = (Z/Z_{\mathbf{r}})(3/\langle r^2\rangle_0^3)^{1/2}(1/2\pi)^{3/2}\times \exp(-3r^2/2\langle r^2\rangle_0)(1 + \alpha_1\eta_2 + \alpha_2\eta_4 + \alpha_3\eta_6 + \alpha_4\eta_8 + \beta_1 g_4 + \beta_2 g_6 + \beta_3 g_8) \quad (17)$$

where

$$\alpha_1 \equiv 3(3x^2 - r^2)/\langle r^2\rangle_0$$

$$\alpha_2 \equiv 3^2\left(\frac{7}{3} - \frac{r^2}{\langle r^2\rangle_0}\right)(3x^2 - r^2)/\langle r^2\rangle_0$$

$$\alpha_3 \equiv 3^3\left(7 - 6\frac{r^2}{\langle r^2\rangle_0} + \frac{r^4}{\langle r^2\rangle_0^2}\right)(3x^2 - r^2)/\langle r^2\rangle_0$$

$$\alpha_4 \equiv 3^4\left(\frac{77}{3} - 33\frac{r^2}{\langle r^2\rangle_0} + 11\frac{r^4}{\langle r^2\rangle_0^2} - \frac{r^6}{\langle r^2\rangle_0^3}\right)(3x^2 - r^2)/\langle r^2\rangle_0 \quad (18)$$

and

$$\beta_1 \equiv 15 - 30\frac{r^2}{\langle r^2\rangle_0} + 9\frac{r^4}{\langle r^2\rangle_0^2}$$

$$\beta_2 \equiv 105 - 315\frac{r^2}{\langle r^2\rangle_0} + 189\frac{r^4}{\langle r^2\rangle_0^2} - 27\frac{r^6}{\langle r^2\rangle_0^3}$$

$$\beta_3 \equiv 945 - 3780\frac{r^2}{\langle r^2\rangle_0} + 3402\frac{r^4}{\langle r^2\rangle_0^2} - 972\frac{r^6}{\langle r^2\rangle_0^3} + 81\frac{r^8}{\langle r^2\rangle_0^4} \quad (19)$$

The ratio $Z_{\mathbf{r}}/Z$ is equal to the distribution function $W(\mathbf{r})$ of the chain end-to-end vector. The latter may be expressed as a series expansion as derived by Nagai,[5] which, upon substitution of the variables defined in eqs 15 and 19, takes the simple form

$$Z_{\mathbf{r}}/Z = W(\mathbf{r}) = (2\pi\langle r^2\rangle_0/3)^{-3/2}\times \exp\{-3r^2/2\langle r^2\rangle_0\}\,[1 + \beta_1 g_4 + \beta_2 g_6 + \beta_3 g_8 + \ldots] \quad (20)$$

When eq 20 is inserted into eq 17, the following expression is obtained for the average of $\langle\cos^2\theta\rangle_{\mathbf{r}}$ of the unit

vector **m**

$$\langle \cos^2 \theta \rangle_{\mathbf{r}} = \frac{1}{3}(1 + \beta_1 g_4 + \beta_2 g_6 + \beta_3 g_8 + \ldots)^{-1}(1 + \alpha_1 \eta_2 + \alpha_2 \eta_4 + \alpha_3 \eta_6 + \alpha_4 \eta_8 + \beta_1 g_4 + \beta_2 g_6 + \beta_3 g_8 + \ldots) \quad (21)$$

Equation 21 may be approximated by expanding the first term in parentheses as

$$\langle \cos^2 \theta \rangle_{\mathbf{r}} \cong \frac{1}{3}(1 - \beta_1 g_4 - \beta_2 g_6 - \beta_3 g_8)(1 + \alpha_1 \eta_2 + \alpha_2 \eta_4 + \alpha_3 \eta_6 + \alpha_4 \eta_8 + \beta_1 g_4 + \beta_2 g_6 + \beta_3 g_8) = \frac{1}{3} + (1 - \beta_1 g_4 - \beta_2 g_6 - \beta_3 g_8)\sum_{i=1}^{4}[\alpha_i \eta_{2i}/3] \quad (22)$$

Step 2. Calculation of $\langle \cos^2 \theta \rangle$. The expression given by eq 22 is an average for a single chain of the network having its two ends fixed. For relating the segmental orientation to that observed in experiments, we have to average eq 22 over all orientations and magnitudes of the end-to-end chain vectors. In eq 22 the coefficients η_i and g_i include statistical averages that have already been performed, as is apparent from eqs 14 and 15. Averaging over the ensemble of chains has therefore to be carried out only for the terms comprising α_i and β_i. The latter includes ratios of the form $r^m/\langle r^2 \rangle_0^{m/2}$, and α_i includes both those ratios and other terms of the form $3x^2/\langle x^2 \rangle_0 - r^2/\langle r^2 \rangle_0$. If the powers of r are written in terms of the x, y, and z components, a representative term whose ensemble average has to be taken will have the form $x^p y^q z^r$, where x, y, and z are the components of the end-to-end vector in the deformed state. According to the affine deformation assumption, they are related to those in the undeformed state by

$$x^p y^q z^r = \lambda_x{}^p \lambda_y{}^q \lambda_z{}^r x_0{}^p y_0{}^q z_0{}^r \quad (23)$$

Here λ_x, λ_y, and λ_z are the x, y, and z components of λ. When the polar and azimuthal angles of a chain end-to-end vector are represented by ϑ and φ, the undeformed components may in turn be expressed as

$$x_0 = r_0 \cos \vartheta$$

$$y_0 = r_0 \sin \vartheta \cos \varphi$$

$$z_0 = r_0 \sin \vartheta \sin \varphi \quad (24)$$

Substitution of eq 24 into eq 23 and averaging over both r_0 and the trigonometric functions leads to

$$\langle x^p y^q z^r \rangle = \lambda_x{}^p \lambda_y{}^q \lambda_z{}^r \langle r^{p+q+r} \rangle_0 Q(p,q,r) \quad (25)$$

where

$$Q(p,q,r) = (4\pi)^{-1} \int_{\varphi=0}^{2\pi} \int_{\vartheta=0}^{\pi} \cos^p \vartheta \sin^{q+r+1} \vartheta \cos^q \varphi \sin^r \varphi \, d\varphi \, d\vartheta \quad (26)$$

The application of the above integrations to isotropic, unperturbed chains leads to the averages of unperturbed dimension and of α_i, β_i, and $\alpha_i \beta_j$. These are listed in the Appendix. These averages are inserted into eq 22 to yield the average $\langle \cos^2 \theta \rangle$ over all **r**. It is convenient to organize the latter on the basis of increasing powers of λ. Following the arguments given by Nagai[3] and Flory,[4] it can be shown that the coefficients g_i and η_i scale with the number n of segments in a chain as follows:

$$g_4, \eta_2 \sim n^{-1}$$

$$g_6, g_8, \eta_4, \eta_6 \sim n^{-2} \quad (27)$$

$$\eta_8 \sim n^{-3}$$

Accordingly, $\langle \cos^2 \theta \rangle$ may be rearranged as

$$\langle \cos^2 \theta \rangle = \frac{1}{3}\Big[1 + D_1(\lambda^2 - \lambda^{-1}) + D_2\Big(\lambda^4 + \frac{1}{3}\lambda - \frac{4}{3}\lambda^{-2}\Big) + D_3\Big(\lambda^6 + \frac{3}{5}\lambda^3 - \frac{8}{5}\lambda^{-3}\Big) + D_4\Big(\lambda^8 + \frac{5}{7}\lambda^5 + \frac{12}{35}\lambda^2 - \frac{8}{35}\lambda^{-1} - \frac{64}{35}\lambda^{-4}\Big) + \ldots\Big] \quad (28)$$

where

$$D_1 = 2\eta_2 + 14\eta_4 + 126\eta_6 + 1386\eta_8 - 30\eta_2 g_4 - 210\eta_2 g_6 - 1890\eta_2 g_8 - 210\eta_4 g_4 - 1890\eta_6 g_4$$

$$D_2 = -\frac{18}{5}(\eta_4 + 18\eta_6 + 297\eta_8 - 10\eta_2 g_4 - 105\eta_2 g_6 - 1260\eta_2 g_8 - 85\eta_4 g_4 - 900\eta_6 g_4)\frac{\langle r^4 \rangle_0}{\langle r^2 \rangle_0{}^2}$$

$$D_3 = \frac{54}{7}(\eta_6 + 33\eta_8 - \eta_2 g_4 - 21\eta_2 g_6 - 378\eta_2 g_8 - 17\eta_4 g_4 - 258\eta_6 g_4)\frac{\langle r^6 \rangle_0}{\langle r^2 \rangle_0{}^3}$$

$$D_4 = 18(\eta_2 g_6 + 36\eta_2 g_8 + \eta_4 g_4 + 28\eta_6 g_4)\frac{\langle r^8 \rangle_0}{\langle r^2 \rangle_0{}^4} \quad (29)$$

It should be noted that, in eq 29, the leading term of D_1 is of order n^{-1}, those of D_2 and D_3 are of order n^{-2}, and that of D_4 is of order n^{-3}.

Orientation Function. The second Legendre function S, also termed as the orientation function, is defined by

$$S = [3\langle \cos^2 \theta \rangle - 1]/2 \quad (30)$$

Substitution of eq 28 into eq 30 yields

$$S = \frac{1}{2}\Big[D_1(\lambda^2 - \lambda^{-1}) + D_2\Big(\lambda^4 + \frac{1}{3}\lambda - \frac{4}{3}\lambda^{-2}\Big) + D_3\Big(\lambda^6 + \frac{3}{5}\lambda^3 - \frac{8}{5}\lambda^{-3}\Big) + D_4\Big(\lambda^8 + \frac{5}{7}\lambda^5 + \frac{12}{35}\lambda^2 - \frac{8}{35}\lambda^{-1} - \frac{64}{35}\lambda^{-4}\Big) + \ldots\Big] \quad (31)$$

Inasmuch as the next coefficient D_5 will include terms of the order n^{-3}, eq 31 cannot be regarded as complete up to the third order. Accordingly, calculations in the ensuing section are confined only to the first- and second-order approximations.

The orientation function in the small deformation limit may be obtained from eq 31 by factoring out the conventional small-strain expression $\epsilon = \lambda - 1$ and letting $\lambda = 1$. The result takes the form

$$S = \frac{3}{2}\Big(D_1 + \frac{7}{3}D_2 + \frac{21}{5}D_3 + \frac{33}{5}D_4\Big)\epsilon \quad (32)$$

Results of Calculations and Discussion

Calculations were performed for polyethylene (PE) for a quantitative assessment of the relative importance of

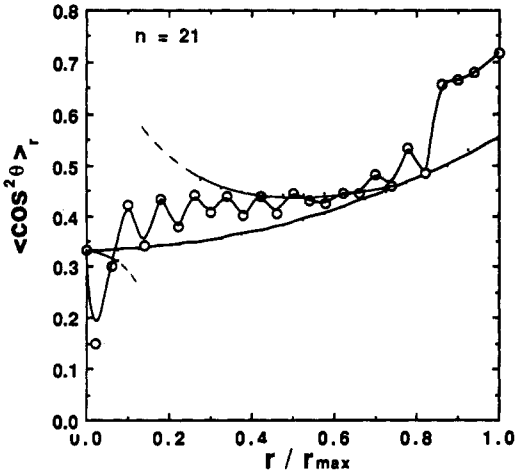

Figure 3. Dependence of $\langle\cos^2\theta\rangle_r$ on r/r_{max} for $n = 21$. The circles are results from MC simulations. The curve through the points is drawn to guide the eye. The lower solid curve is theoretically obtained by using the first-order approximation. The discontinuous curve is found from eq 21. The discontinuous portion is indicated by the dashed curve.

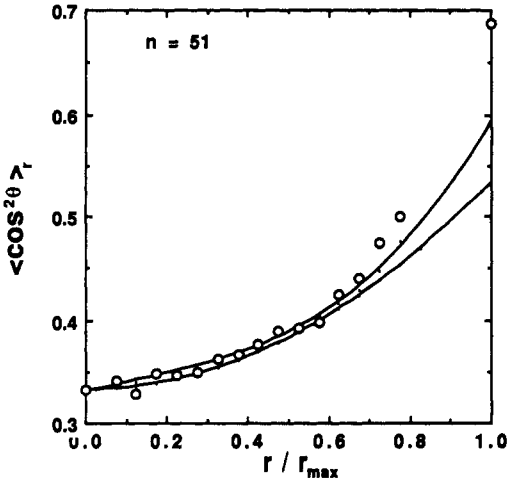

Figure 4. Dependence of $\langle\cos^2\theta\rangle_r$ on r/r_{max} for $n = 51$. The circles are results from MC simulations. The lower solid curve is obtained by using the first-order approximation. The upper curve is found from eq 21.

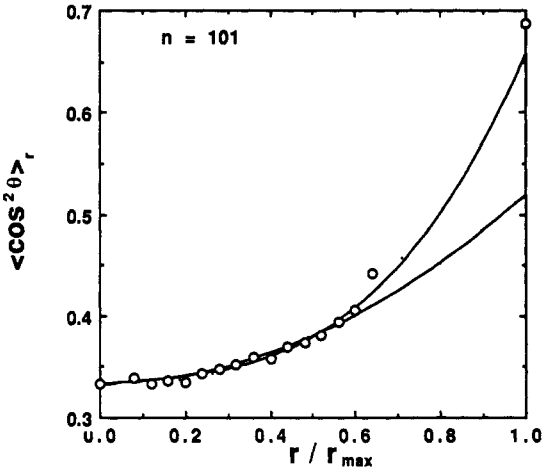

Figure 5. Dependence of $\langle\cos^2\theta\rangle_r$ on r/r_{max} for $n = 101$. The circles are results from MC simulations. The lower solid curve is obtained by using the first-order approximation. The upper curve is found from eq 21.

higher order approximations, in the evaluation of average orientations. Calculations involve two major steps in parallel with the theoretical presentation above: First, chains with constant **r** have been explored. The exact dependence of $\langle\cos^2\theta\rangle_r$ on **r** has been determined from Monte Carlo simulations and compared with the predictions of eq 21. Second, all network chains have been considered, and the degree of orientation has been investigated as a function of extension ratio, by adopting both first- and second-order dependences on $1/n$, for comparison. The results from the two sets of calculations are separately presented and discussed in the following.

Orientation in a Chain with Fixed r. Monte Carlo (MC) simulations are used in the present work for two purposes: First, it is possible to obtain an exact value for $\langle\cos^2\theta\rangle_r$ as a function of **r**, provided that a sufficiently large number of chains is generated. Second, MC chains are used for the determination of moments of the form $\langle r^{2m}\cos^2\theta\rangle_0$ and $\langle r^{2m}\rangle_0$, with $m = 1$–4, which will be required for the evaluation of η_i and g_j in eq 21. In particular, evaluation of averages with the usual generator matrix technique of the rotational isomeric state formalism is prohibitively difficult when m is larger than 2, and MC calculations are indispensable.

Monte Carlo chains are generated by the conventional rotational isomeric state approach based on distinct conditional probabilities for each bond, using the well-established energy and geometry parameters of PE.[4] They are classified according to the magnitude of their end-to-end vectors, and the average square cosine of the angle between the central bond and the vector **r** is evaluated for each subset of chains lying in a given interval of $r \pm \Delta r$. The resulting $\langle\cos^2\theta\rangle_r$ values are plotted as a function of r/r_{max} in Figures 3–5, for the respective cases $n = 21$, 51, and 101. r_{max} refers to the maximum end-to-end separation, i.e., that of the all-trans configuration. The final point at $r/r_{max} = 1$ is calculated for the central bond in a fully extended chain of $n = 21$, 51, and 101 bonds as $\langle\cos^2\theta\rangle_r = 0.717$, 0.699, and 0.694, respectively. Bond supplemental angles are taken as $\theta = 68°$. Results from MC simulations for each of the successive intervals are shown by the empty circles. In order to end up with a reliable number of chains in each interval, generation of a set of $\sim 10^5$ chains is required for a given n. It is observed in Figure 3 that $\langle\cos^2\theta\rangle_r$ values for $n = 21$, which are connected by a curve to guide the eye, are subject to considerable fluctuations. The latter are not due to uncertainties or scattering in the properties of the generated chains but to a systematic reproducible effect that may be attributed to small chain length. Similar fluctuations, though considerably weakened in amplitude, are discernible in longer chains, as may be seen in Figures 4 and 5.

For comparative purposes, the theoretical curves obtained with (i) the first-order approximation where $\langle\cos^2\theta\rangle_r = {}^1/_3 + \alpha_1\eta_2/3$ and (ii) the more complete expression given by eq 21 are shown in Figures 3–5. Comparison of the theory with MC simulations is made possible by identifying the direction of the end-to-end vector with the x axis. In all cases the lower curves represent the first-order approximation whereas the upper curves are obtained from eq 21. The extrapolation of the latter to $r/r_{max} = 1$ has been carried out with the help of best fitting third-order polynomials. From the observation of Figures 4 and 5, it is noted that in the case of longer chains the two approaches are both satisfactory, although eq 21 exhibits a better agreement with the real behavior, which is indicated by MC simulations. The deviation between the two approaches is particularly apparent at more extended configurations. For $n = 21$, however, the first-order approximation curve lies definitely below the MC simu-

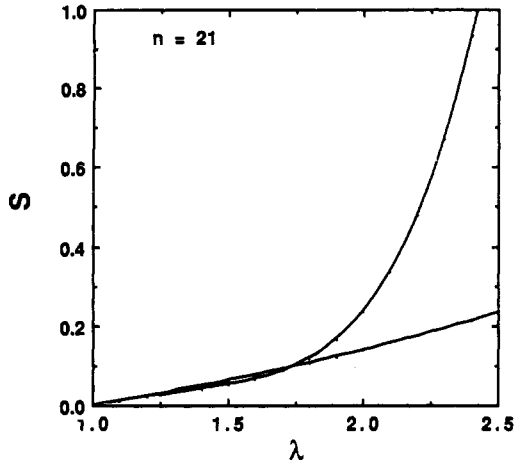

Figure 6. Dependence of the orientation function, S, on the extension ratio, λ, for a chain with 21 bonds. The lower curve is obtained from the linear expression given by eq 35. The upper curve is from the second-order expression obtained by inserting the coefficients given by eq 34 into eq 31.

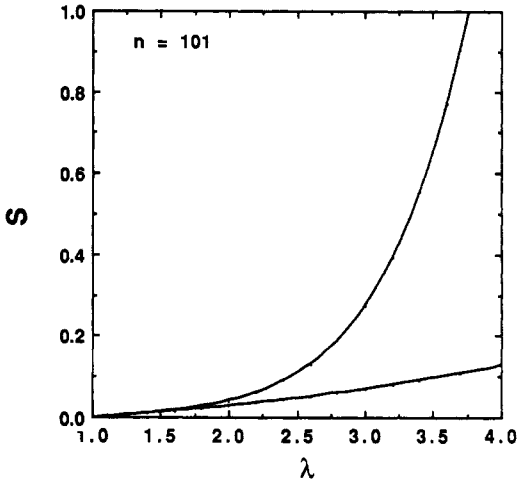

Figure 7. Dependence of the orientation function, S, on the extension ratio, λ, for a chain with 101 bonds. See figure capture for Figure 6.

lation points, regardless of r/r_{max}, and is not adequate for data interpretation. In this respect, approach ii follows more closely the MC simulations, apart from a singularity near $r/r_{max} = 0.2$, due to the vanishing of the denominator in eq 21. This region is shown by the dashed portion of the curve.

Orientation as a Function of λ. The dependence of S on λ is shown in Figure 6 for $n = 21$. The solid curve is obtained from eq 31 by retaining the linear term only, i.e., by adopting

$$D_1 = 2\eta_2$$

$$D_2 = D_3 = D_4 = 0 \tag{33}$$

The dashed curve in Figure 6 is obtained for the second-order approximation by the use of the following expressions for the D_i's in eq 31

$$D_1 = 2\eta_2 + 14\eta_4 + 126\eta_6 - 30\eta_2 g_4$$

$$D_2 = -\frac{18}{5}(\eta_4 + 18\eta_6 - 10\eta_2 g_4)\frac{\langle r^4\rangle_0}{\langle r^2\rangle_0^2}$$

$$D_3 = \frac{54}{7}(\eta_6 - \eta_2 g_4)\frac{\langle r^6\rangle_0}{\langle r^2\rangle_0^3}$$

$$D_4 = 0 \tag{34}$$

The results of the first- and second-order approximations shown in Figure 6 for $n = 21$ are very close to each other for $1 < \lambda < 1.75$. In this range, the second-order approximation predicts slightly smaller S values than the linear one. Above $\lambda = 1.75$, however, the second-order approximation for S increases very sharply to full orientation at about $\lambda = 2.8$. It may be concluded from Figure 6 that for polyethylene-like chains as short as 20 bonds, the first-order approximation to orientation given by the very simple expression

$$S = \frac{1}{2}D_1(\lambda^2 - \lambda^{-1}) \tag{35}$$

is satisfactory for relatively small strains. However, the identification of the front factor in eq 35 with the Kuhn expression of $1/5N$, with N indicating the number of Kuhn segments in the network chain, is not acceptable as has been demonstrated previously.[5] For a polyethylene chain of $n = 21$ bonds, one Kuhn segment contains about 10–22 C–C bonds, depending on the definition of the Kuhn length.[4,6] Thus, $1/5N$ assumes values between 0.1 and 0.2 while the present calculations predict a value of 0.02 for $D_1/2$.

Results of calculations of S for $n = 101$ are shown in Figure 7 as a function of λ. The upper curve obtained by the second-order approximation departs from the results of the linear approximation, the lower curve, around $\lambda = 2$. $D_1/2$ is 0.004 for this chain and deviates strongly from the Kuhn approximation.

It may be concluded from the form of eq 31 that S has to converge to the expression given by eq 35 in the limit of very large n. The strong deviation of the two curves from each other in Figure 7 indicates, however, that $n = 101$ is a value much lower than that required for eq 35 to be strictly valid. It may be interesting to note the abruptness of the deviation of the second-order curves in Figures 6 and 7 from the respective first-order ones. The marked rise of the curves in the second-order approximation results from the dominance of the λ^6 term with increasing extension. This type of behavior at higher strains is distinctly exhibited by the recent results of infrared dichroism measurements in high *cis*-1,4-polybutadiene networks.[7]

A comparison of eq 28 with the results of Roe and Krigbaum[8] for finite freely jointed chains shows that the functions containing the λ's are identical in the two works and both formulations show strong resemblances. However, the coefficient D_3 of eq 28 is of order n^{-2} whereas the corresponding coefficient in the work of Roe and Krigbaum is of order n^{-3}. It may thus be concluded that the present study does not converge to that of Roe and Krigbaum in the limit of freely jointed chains.

Orientation in the Small-Strain Limit. Calculations of the values of S/ϵ from eq 32 by retaining only terms of order n^{-1} lead to 0.1176, 0.0525, and 0.0243 for $n = 21$, 51, and 101, respectively. When terms of order n^{-2}, i.e., second-order terms, are included, the above values become, respectively, 0.1253, 0.0546, and 0.0255. This comparison shows that the contributions of the second-order terms to S/ϵ are 6.6%, 4.0%, and 5.1% for $n = 21$, 51, and 101, respectively. Thus it may be concluded that, in the small-strain limit, the term S/ϵ, which may be referred to as the

orientational modulus, is satisfactorily represented by

$$S/\epsilon = \frac{3}{10}\left(\frac{3\langle r^2 \cos^2 \Phi\rangle_0}{\langle r^2\rangle_0} - 1\right) \tag{36}$$

The above equation is particularly useful in interpreting results from infrared dichroism experiments recently developed by Noda et al.,[1] which allow for very precise determination of S/ϵ.

Acknowledgment. Financial support from the National Science Foundation Program "Science in Developing Countries" (Grant INT-8903327) is gratefully acknowledged.

Appendix

With performance of the integrations indicated in eq 26, the averages shown in eq 25 are obtained up to the eighth order as

$$\langle x^2\rangle_0 = \langle y^2\rangle_0 = \langle z^2\rangle_0 = \langle r^2\rangle_0/3$$

$$\langle x^4\rangle_0 = \langle y^4\rangle_0 = \langle z^4\rangle_0 = \langle r^4\rangle_0/5$$

$$\langle x^6\rangle_0 = \langle y^6\rangle_0 = \langle z^6\rangle_0 = \langle r^6\rangle_0/7$$

$$\langle x^8\rangle_0 = \langle y^8\rangle_0 = \langle z^8\rangle_0 = \langle r^8\rangle_0/9$$

$$\langle x^2y^2\rangle_0 = \langle x^2z^2\rangle_0 = \ldots = \langle r^4\rangle_0/15$$

$$\langle x^2y^4\rangle_0 = \langle x^2z^4\rangle_0 = \ldots = \langle r^6\rangle_0/35$$

$$\langle x^2y^6\rangle_0 = \langle x^2z^6\rangle_0 = \ldots = \langle r^8\rangle_0/63$$

$$\langle x^4y^4\rangle_0 = \langle x^4z^4\rangle_0 = \ldots = \langle r^8\rangle_0/105$$

$$\langle x^2y^2z^2\rangle_0 = \langle r^6\rangle_0/60$$

$$\langle x^4y^2z^2\rangle_0 = \langle y^4x^2z^2\rangle_0 = \ldots = \langle r^8\rangle_0/315 \tag{A-1}$$

The terms not shown in eq A-1 are readily obtained from symmetry. The use of these averages leads to the following averages of α_i, β_i, and $\alpha_i\beta_j$

$$\langle\alpha_1\rangle = 2\Lambda_2$$

$$\langle\alpha_2\rangle = 14\Lambda_2 - \frac{6}{5}\frac{\langle r^4\rangle_0}{\langle r^2\rangle_0^2}\Lambda_4$$

$$\langle\alpha_3\rangle = \Lambda_2 - \frac{108}{5}\frac{\langle r^4\rangle_0}{\langle r^2\rangle_0^2}\Lambda_4 + \frac{54}{7}\frac{\langle r^6\rangle_0}{\langle r^2\rangle_0^3}\Lambda_6$$

$$\langle\alpha_4\rangle = 1386\Lambda_2 - \frac{1782}{5}\frac{\langle r^4\rangle_0}{\langle r^2\rangle_0^2}\Lambda_4 + \frac{1782}{7}\frac{\langle r^6\rangle_0}{\langle r^2\rangle_0^3}\Lambda_6 - 18\frac{\langle r^8\rangle_0}{\langle r^2\rangle_0^4}\Lambda_8$$

$$\langle\alpha_1\beta_1\rangle = 30\Lambda_2 - 12\frac{\langle r^4\rangle_0}{\langle r^2\rangle_0^2}\Lambda_4 + \frac{54}{7}\frac{\langle r^6\rangle_0}{\langle r^2\rangle_0^3}\Lambda_6$$

$$\langle\alpha_1\beta_2\rangle = 210\Lambda_2 - 378\frac{\langle r^4\rangle_0}{\langle r^2\rangle_0^2}\Lambda_4 + 162\frac{\langle r^6\rangle_0}{\langle r^2\rangle_0^3}\Lambda_6 - 18\frac{\langle r^8\rangle_0}{\langle r^2\rangle_0^4}\Lambda_8$$

$$\langle\alpha_1\beta_3\rangle = 1890\Lambda_2 - 4536\frac{\langle r^4\rangle_0}{\langle r^2\rangle_0^2}\Lambda_4 + 2916\frac{\langle r^6\rangle_0}{\langle r^2\rangle_0^3}\Lambda_6 - 648\frac{\langle r^8\rangle_0}{\langle r^2\rangle_0^4}\Lambda_8$$

$$\langle\alpha_2\beta_1\rangle = 210\Lambda_2 - 306\frac{\langle r^4\rangle_0}{\langle r^2\rangle_0^2}\Lambda_4 + \frac{918}{7}\frac{\langle r^6\rangle_0}{\langle r^2\rangle_0^3}\Lambda_6 - 18\frac{\langle r^8\rangle_0}{\langle r^2\rangle_0^4}\Lambda_8$$

$$\langle\alpha_3\beta_1\rangle = 1890\Lambda_2 - 3240\frac{\langle r^4\rangle_0}{\langle r^2\rangle_0^2}\Lambda_4 + \frac{13932}{7}\frac{\langle r^6\rangle_0}{\langle r^2\rangle_0^3}\Lambda_6 - 504\frac{\langle r^8\rangle_0}{\langle r^2\rangle_0^4}\Lambda_8 \tag{A-2}$$

where

$$\Lambda_2 = \lambda^2 - \lambda^{-1}$$

$$\Lambda_4 = 3\lambda^4 + \lambda - 4\lambda^{-2}$$

$$\Lambda_6 = \lambda^6 + \frac{3}{5}\lambda^3 - \frac{8}{5}\lambda^{-3}$$

$$\Lambda_8 = \lambda^8 + \frac{5}{7}\lambda^5 + \frac{12}{35}\lambda^2 - \frac{8}{35}\lambda^{-1} - \frac{64}{35}\lambda^{-4} \tag{A-3}$$

References and Notes

(1) (a) Noda, I.; Dowrey, A. E.; Marcott, C. (i) *Fourier Transform Infrared Characterization*; Ed.; M., Ishida, Plenum: New York, 1987. (b) Noda, I.; Dowrey, A. E.; Marcott, C. *Appl. Spectrosc.* **1988**, *42*, 203.
(2) Dubault, A.; Deloche B.; Herz, J. *Polymer* **1984**, *25*, 1405.
(3) Nagai, K. *J. Chem. Phys.* **1964**, *40*, 2818.
(4) Flory, P. J. *Statistical Mechanics of Chain Molecules*; Interscience: New York, 1969.
(5) Erman, B.; Bahar, I. *Macromolecules* **1988**, *21*, 457.
(6) Yoon, D. Y.; Flory, P. J. *J. Chem. Phys.* **1974**, *61*, 5366.
(7) Amram, B.; Bokobza, L.; Monnerie, L.; Queslel, J. P. *Polymer* **1988**, *29*, 1155.
(8) Roe, R.-J.; Krigbaum, W. R. *J. Appl. Phys.* **1964**, *35*, 2215.

Registry No. PE, 9002-88-4.